Effects of simplified enthalpy relations on the prediction of heat transfer during solidification of a lead-tin alloy

M. C. Schneider and C. Beckermann

Department of Mechanical Engineering, University of Iowa, Iowa City, IA, USA

An investigation into the effects of enthalpy functions that vary with both concentration and temperature on the prediction of heat transfer during solidification using a volume-averaged mixture energy equation is presented. Results are presented for the solidification of a Pb-20 wt.% Sn alloy in a semi-infinite domain using both the Lever Rule and Scheil models to relate temperature and volume fraction. The effects of simplifying the enthalpy relations so that the derivatives of the phase enthalpies with respect to temperature and concentration are constant or zero are examined. The resulting predictions all underestimate the movement of the eutectic and liquidus isotherms in comparison with fully variable enthalpy terms. The additional simplifications of linearizing the phase diagram and using the same properties for the α-phase and eutectic solids introduce a small improvement in the predictions. In addition, the consequences of neglecting the effects of microscopic concentration profiles in the solid on the solid enthalpy are investigated, and the resulting predictions overestimate the movement of the eutectic and liquidus isotherms. The results should serve as an estimation of the magnitude of the differences in the modelling of heat transfer during solidification introduced by simplifying the enthalpy relations or ignoring microscopic concentration variations within the solid.

Keywords: solidification, binary alloy, volume averaging, enthalpy function

Introduction

In modelling the heat transfer that occurs during the solidification of alloys, many assumptions are often made to simplify the analysis. One of the most common simplifications is to assume that the enthalpies of the solid and liquid phases are simple linear functions of the temperature. It has been shown, however, that the phase enthalpies should instead be treated as state functions that vary with both temperature and concentration.[1] For example, the liquid enthalpy may actually increase as the temperature is reduced during solidification owing to the changes in concentration that occur. In addition, the difference in the interfacial liquid and solid enthalpies, or heat of fusion, is not a constant and may in fact increase by over 50% during alloy solidification.[1] Furthermore, the effects of the differences between the enthalpies of the primary solid and the eutectic solid phases are often not taken into account.

A recent development in the modelling of solidification is that volume-averaging procedures have been used to rigorously derive macroscopic models of solidification.[2,3] The advantage of volume averaging is that it provides information about the relationship between the macroscopic (averaged) variables and the microscopic (local) variables.[3] This is important because thermodynamic state functions are valid only for the local variables. These functions are not valid for the averaged quantities of a phase, for example, because of microsegregation. Therefore the neglect of property variations on a microscopic scale can affect the predictions of a macroscopic model.

The purpose of the present investigation into the modelling of heat transfer during solidification is twofold. First, we investigate the effects of using complete enthalpy expressions that are functions of both temperature and concentration. Second, we observe the results of neglecting microscopic property variations in determining the enthalpy. As a simple example, we consider the modelling of heat transfer during the solidification of a lead-tin alloy in a semi-infinite domain without fluid flow.

Analysis

Energy equation

Because of the presence of complicated interfacial structures, such as dendrites, that characterize the solidification of metallic alloys, it is impractical to solve

Address reprint requests to Dr. Beckermann at the Department of Mechanical Engineering, University of Iowa, Iowa City, IA 52242, USA.

Received 19 December 1990; revised 29 July 1991; accepted 14 August 1991

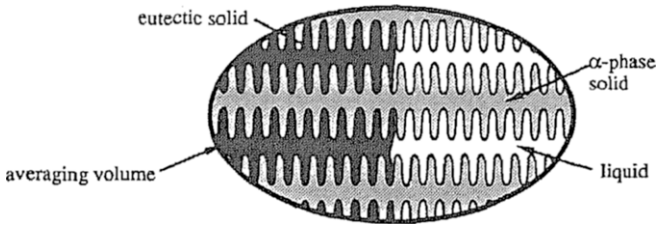

Figure 1. A typical averaging volume that includes eutectic solid, α-phase solid, and liquid

the exact conservation equations on a microscopic scale. Instead, macroscopic models are utilized that can be derived by averaging the exact equations for each phase over a finite sized averaging volume. This volume, shown in *Figure 1*, is much smaller than the system and large in comparison to the interfacial structures. By adding up the averaged equations for each phase a macroscopic mixture equation is obtained.[2,3] If we assume no fluid flow and no net flow of solute into or out of the averaging volume, the mixture energy equation can be written as

$$\frac{\partial}{\partial t}[\epsilon_l\rho_l\langle h_l\rangle^l + \epsilon_\alpha\rho_\alpha\langle h_\alpha\rangle^s + \epsilon_\gamma\rho_\gamma\langle h_\gamma\rangle^\gamma] = \nabla\cdot\{\epsilon_l k_l\nabla\langle T_l\rangle^l + \epsilon_\alpha k_\alpha\nabla\langle T_\alpha\rangle^\alpha + \epsilon_\gamma k_\gamma\nabla\langle T_\gamma\rangle^\gamma\} \quad (1)$$

Note that the assumption of no net flow of solute into or out of the averaging volume implies that there is no macroscopic heat flux caused by interdiffusion and the Dufour effect. Equation (1) accounts for the presence of three phases, with the liquid phase denoted by a subscript l, the primary alpha phase solid denoted by a subscript α, and the gamma phase solid (which forms in combination with the α-phase solid during the eutectic reaction) denoted by a subscript γ. The intrinsic volume average of some quantity Ψ_k of phase k is defined as

$$\langle\Psi_k\rangle^k = \frac{1}{V_k}\int_{V_0} X_k\Psi_k\,dV \quad (2)$$

where X_k is a phase function that is equal to unity in phase k and zero elsewhere, V_k is the volume occupied by phase k within the averaging volume, and V_0 is the size of the averaging volume. Since the volume averaging is performed for arbitrary volume fractions, equation (1) is equally valid for the fully solid, mush, and fully liquid regions. The volume fractions are related by

$$\epsilon_\alpha + \epsilon_\gamma + \epsilon_l = 1 \quad (3)$$

The effective thermal conductivities, k_k, in equation (1) account for the presence of the other phases but, owing to lack of information, are assumed to be equal to the thermal conductivities of each separate phase. These conductivities are functions of concentration and temperature but are assumed to be constant to allow for an independent investigation into the effects of the dependence of the phase enthalpies on temperature and concentration.

Particular care must be taken in relating the average enthalpies and their derivatives to the average temperature and concentration. The microscopic (local) enthalpy can be expressed as a function of the microscopic (local) temperature and concentration through a thermodynamic state function of the general form

$$h_k = h_k(T_k, C_k) \quad (4)$$

It is important to realize that equation (4) might not be valid for the corresponding average quantities because of microscopic variations of T_k and C_k within the averaging volume. A detailed discussion of the development of an average enthalpy relation that is a function of the average temperature and concentration is provided in the section on enthalpy relations. The outcome of this discussion is that the average enthalpy of a phase can be expressed as a function of the average temperature and concentration so that the differential of the enthalpy is given by

$$d\langle h_k\rangle^k = \left.\frac{\partial\langle h_k\rangle^k}{\partial\langle T_k\rangle^k}\right|_{\langle C_k\rangle^k} d\langle T_k\rangle^k + \left.\frac{\partial\langle h_k\rangle^k}{\partial\langle C_k\rangle^k}\right|_{\langle T_k\rangle^k} d\langle C_k\rangle^k \quad (5)$$

The assumption that the phases within the averaging volume are in thermal equilibrium, that is,

$$\langle T_\alpha\rangle^\alpha = \langle T_\gamma\rangle^\gamma = \langle T_l\rangle^l = T \quad (6)$$

is reasonable for most solidification processes involving metallic alloys. If we utilize equations (5) and (6) and assume constant but unequal densities in each phase, the energy equation is rewritten as

$$\left[\rho_l\epsilon_l\left.\frac{\partial\langle h_l\rangle^l}{\partial T}\right|_{\langle C_l\rangle^l} + \rho_\alpha\epsilon_\alpha\left.\frac{\partial\langle h_\alpha\rangle^\alpha}{\partial T}\right|_{\langle C_\alpha\rangle^\alpha} + \rho_\gamma\epsilon_\gamma\left.\frac{\partial\langle h_\gamma\rangle^\gamma}{\partial T}\right|_{\langle C_\gamma\rangle^\gamma}\right]\frac{\partial T}{\partial t} + \left[\rho_l\epsilon_l\left.\frac{\partial\langle h_l\rangle^l}{\partial\langle C_l\rangle^l}\right|_T\frac{\partial\langle C_l\rangle^l}{\partial t} + \rho_\alpha\epsilon_\alpha\left.\frac{\partial\langle h_\alpha\rangle^\alpha}{\partial\langle C_\alpha\rangle^\alpha}\right|_T\frac{\partial\langle C_\alpha\rangle^\alpha}{\partial t} + \rho_\gamma\epsilon_\gamma\left.\frac{\partial\langle h_\gamma\rangle^\gamma}{\partial\langle C_\gamma\rangle^\gamma}\right|_T\frac{\partial\langle C_\gamma\rangle^\gamma}{\partial t}\right] = \nabla\cdot\{[\epsilon_l k_l + \epsilon_\alpha k_\alpha + \epsilon_\gamma k_\gamma]\nabla T\} - \left[\rho_l\langle h_l\rangle^l\frac{\partial\epsilon_l}{\partial t} + \rho_\alpha\langle h_\alpha\rangle^\alpha\frac{\partial\epsilon_\alpha}{\partial t} + \rho_\gamma\langle h_\gamma\rangle^\gamma\frac{\partial\epsilon_\gamma}{\partial t}\right] \quad (7)$$

The term in equation (7) that involves the time derivative of the temperature and the specific heats (derivatives of enthalpy with respect to temperature at constant concentration) is always included in solidification modelling, but the time derivatives of the solid and liquid concentrations (and the derivatives of enthalpy

with respect to concentration at constant temperature) are seldom considered. The last term, involving the time derivative of the solid volume fraction and the phase enthalpies, illustrates the fact that the latent heat (which is a difference in *interfacial* enthalpies) is not directly present in the volume averaged mixture energy equation, but rather the important quantity is the difference in the *average* enthalpies, that is, $\langle h_l \rangle^l - \langle h_\alpha \rangle^\alpha$ or $\langle h_l \rangle^l - \langle h_\gamma \rangle^\gamma$. The average enthalpies are generally not equal to the interfacial enthalpies of a phase because of temperature and concentration variations on a microscopic scale within the averaging volume. Also, note that the assumption of unequal densities in the solid and liquid phases is inconsistent with the assumption of no fluid flow but is included here for its effects on the other thermophysical properties. Furthermore, the densities are also functions of concentration and temperature but are assumed to be constant to allow for an independent investigation into the effects of the temperature and concentration dependence of the enthalpies.

Solid fraction-concentration-temperature relations

In addition to the energy equation, relationships between the solid fractions, the concentrations, and the temperature are needed to close the problem. In solidification modelling, the Lever Rule model and the Scheil model can be used to obtain such relationships.[4] These two models are illustrated in *Figure 2*. Both models make the assumption that the liquid within the averaging volume is well mixed, that is, the concentration is constant throughout the liquid and equal to the interfacial liquid concentration, but the models take two extremes with respect to the solid concentration. In the Lever Rule model the solid has an infinitely large mass diffusivity so that there are no microscopic concentration gradients within the averaging volume. On the other hand, the Scheil model assumes that the solid mass diffusivity is zero so that a microscopic concentration gradient does exist. For most metal alloys the mass diffusivity of the solid is much smaller than that of the liquid, making the Scheil model more realistic.

Because of the assumption of no net solute flow into or out of the averaging volume, the average phase concentrations will always be related to the initial concentration by

$$\epsilon_l \rho_l \langle C_l \rangle^l + \epsilon_\alpha \rho_\alpha \langle C_\alpha \rangle^\alpha + \epsilon_\gamma \rho_\gamma \langle C_\gamma \rangle^\gamma = (\epsilon_l \rho_l + \epsilon_\alpha \rho_\alpha + \epsilon_\gamma \rho_\gamma) C_0 \quad (8)$$

where C_0 is the initial concentration of the liquid in the averaging volume. It is important to realize that equation (8) does not allow for any macrosegregation, that is, the mixture concentration is always equal to the initial concentration. Up to the eutectic point, the interfacial solid and liquid concentrations can be related through the equilibrium phase diagram by

$$C_{\alpha i} = \kappa_\alpha C_{li} \quad (9)$$

where κ_α is the segregation coefficient obtained from the phase diagram and $C_{\alpha i}$ and C_{li} are the interfacial α-phase and liquid concentrations, respectively. Equation (9) assumes the α-phase to be the primary solid forming. With the Lever Rule model, there are no microscopic concentration gradients within the averaging volume, so the average solid and liquid concentrations are also related by

$$\langle C_\alpha \rangle^\alpha = \kappa_\alpha \langle C_l \rangle^l \quad (10)$$

In the Scheil model, on the other hand, the liquid is still assumed to be well mixed, so equation (9) can be rewritten as

$$C_{\alpha i} = \kappa_\alpha \langle C_l \rangle^l \quad (11)$$

However, the average and interfacial concentrations are related through[3,4]

$$d(\epsilon_\alpha \rho_\alpha \langle C_\alpha \rangle^\alpha) = C_{\alpha i}\, d(\epsilon_\alpha \rho_\alpha) \quad (12)$$

Together, equations (11) and (12) provide a relation between the average solid and liquid concentrations in the Scheil model.

Combining equation (8) with equation (10) or with equations (11) and (12) provides a relationship between the solid fraction and the average liquid concentration for the Lever Rule and Scheil models, respectively.

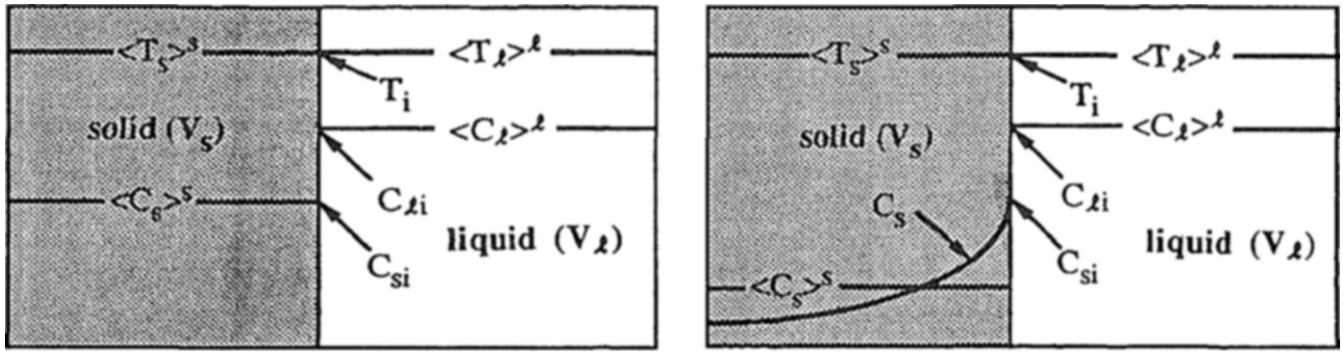

(a) Lever Rule Model (b) Scheil Model

Figure 2. Schematic illustration of the microscopic temperature and concentration profiles assumed in the Lever Rule and Scheil models

The temperature can, in turn, be related to the solid fraction by realizing that the interfacial temperature and the interfacial liquid concentration are related through the liquidus curve of the equilibrium phase diagram, that is,

$$T_i = g(C_{il}) \tag{13}$$

where T_i is the interfacial temperature and g is the equation for the liquidus line. The assumptions of thermal equilibrium and a well-mixed liquid phase within the averaging volume allow this relation to be rewritten as

$$T = g(\langle C_l \rangle^l) \tag{14}$$

Therefore equations (8)–(14) provide a relationship between the solid fraction and the temperature for both the Lever Rule and Scheil models.

These models relate the solid volume fraction to the temperature until the eutectic temperature is reached. After that point the remaining liquid solidifies isothermally at the eutectic temperature from liquid that remains at the eutectic composition. The α- and γ-phase solids that form during the eutectic reaction have constant and uniform concentrations at the values given by the phase diagram, and they form in proportions such that the combination has a mixture concentration equal to the eutectic composition. With the temperature and concentrations known, the solid fractions can be determined iteratively from equation (7).

Enthalpy relations. As was mentioned in the section on the energy equation, care must be taken in relating the average enthalpy to the average temperature and concentration. The local enthalpy is described by equation (4), where h_k is generally a nonlinear function of T_k and C_k. Since the liquid is assumed to be well mixed and thermal equilibrium is assumed to exist within the averaging volume, the use of the intrinsic volume average with equation (4) for the liquid phase yields

$$\langle h_l \rangle^l = \frac{1}{V_l} \int_{V_0} X_l h_l(T_l, C_l) dV = h_l(T, \langle C_l \rangle^l) \tag{15}$$

The assumptions of the Lever Rule model allow a similar treatment for the average α-phase solid enthalpy, that is,

$$\langle h_\alpha \rangle^\alpha = \frac{1}{V_\alpha} \int_{V_0} X_\alpha h_\alpha(T_\alpha, C_\alpha) dV = h_\alpha(T, \langle C_\alpha \rangle^\alpha) \tag{16}$$

For the Scheil model, however, a microscopic concentration profile exists in the solid within the averaging volume. In this case the use of the *intrinsic* volume average with an enthalpy function that is nonlinear in concentration will not result in an equation of the form of equation (14). This is due to the fact that the average of the product of two quantities is not equal to the product of the averages, that is,

$$\langle C_\alpha C_\alpha \rangle^\alpha \neq \langle C_\alpha \rangle^\alpha \langle C_\alpha \rangle^\alpha \tag{17}$$

Hence the average α-phase solid enthalpy must theoretically be calculated by performing the integration indicated by equation (2) and taking into account the microscopic concentration profile within the α-phase solid in the averaging volume. Since this concentration profile might not be known or it might be difficult to keep track of in a solidification simulation, it is desirable to develop more direct means of determining the average enthalpy from the average concentration (and temperature). This can be accomplished by linearizing the α-phase solid enthalpy function in concentration. Any nonlinearity in temperature can be retained because the temperature is assumed to be uniform within the averaging volume. The partially linearized enthalpy function, h_α^{lin}, can be used to calculate the average α-phase solid enthalpy via

$$\langle h_\alpha \rangle^\alpha = \frac{1}{V_\alpha} \int_{V_0} X_\alpha h_\alpha^{\text{lin}}(T_\alpha, C_\alpha) dV = h_\alpha^{\text{lin}}(T, \langle C_\alpha \rangle^\alpha) \tag{18}$$

Assuming that no solid state transformations take place, the γ-phase solid that forms during the eutectic reaction will have a uniform and constant concentration. Therefore no linearization of the γ-phase enthalpy relation is necessary. Essentially, the γ-phase enthalpy is a function of temperature only.

Numerical procedure

The energy equation, equation (7), was solved by using a fully implicit control volume finite difference scheme with the Scheil model solid fraction-concentration relation, that is, equation (12), integrated by using four-point Gaussian quadrature. The code was thoroughly tested by using approximate properties of a lead-tin alloy. The grid size of the computational mesh for the results presented here was 0.002 m, and the time step used was 0.1 second. Grid independence was verified by reducing this computational grid by a factor of four. The predictions for the movement of the eutectic and liquidus isotherms for the coarser grid were within 0.05% and 0.3%, respectively, of the predictions for the finer grid. To evaluate the accuracy of the code, the results for a numerical simulation of isothermal solidification without a mushy zone were compared with the Neumann (exact) solution and showed agreement to within 0.2%. Since the following discussion concentrates on the relative differences between various test cases using the same code, rather than on the absolute values of the predictions, the above accuracy was deemed sufficient.

Test cases

To observe the effects of different simplifications on the prediction of heat transfer during solidification, several numerical test cases were performed by using a Pb-20 wt.% Sn alloy. The lead-tin system was chosen because of the availability of thermophysical property data. In particular, the Pb-20 wt.% Sn alloy has been a popular choice for solidification experiments, owing to its relatively low phase change temperatures.[1,5,6]

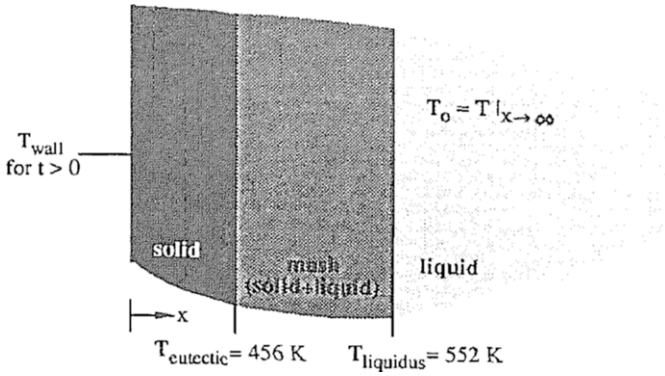

Figure 3. Schematic of semi-infinite domain and boundary conditions (C_0 = 20 wt.% Sn)

Figure 3 shows that each test case involves solidification in a semi-infinite domain with an initial condition of a uniform temperature, T_0, throughout the domain. For times $t > 0$ the temperature at the boundary was fixed at a constant value below the eutectic temperature, T_{wall}.

The equilibrium phase diagram of the lead-tin system is shown in *Figure 4*. The liquidus curve and segregation coefficient of this phase diagram can be approximated by polynomials,[5] that is,

$$\kappa_\alpha = \sum_{j=0}^{n} f_j (C_{il})^j \tag{19}$$

and

$$T_i = \sum_{j=0}^{n} g_j (C_{il})^j \tag{20}$$

where the subscript i indicates an interfacial value. The coefficients f_j and g_j for hypoeutectic alloys (Pb-rich side of the eutectic point) are presented in *Table 1*.

Table 1. Coefficients for segregation coefficient and liquidus curve, equations (19) and (20)[5]

j	f_j	g_j
0	0.8273	600.8
1	-4.2208×10^{-2}	−2.8290
2	1.9680×10^{-3}	2.5088×10^{-2}
3	-5.1866×10^{-5}	-2.7597×10^{-4}
4	6.8075×10^{-7}	—
5	-3.4568×10^{-9}	—

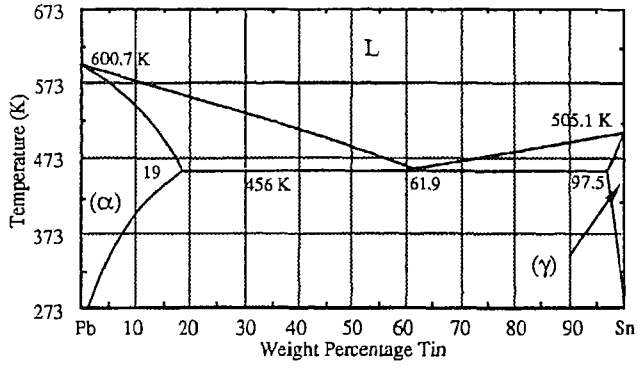

Figure 4. Equilibrium phase diagram of the lead-tin system

The liquidus temperature for the Pb-20 wt.% Sn alloy considered here can be calculated from equation (18) and is found to be 552 K. As *Figure 4* shows, the eutectic temperature and concentration of the lead-tin system are 456 K and 61.9 wt.% Sn, respectively.

Enthalpy relations presented by Poirier and Nandapurkar[1] were used to evaluate the phase enthalpies and are presented here for completeness. The local liquid enthalpy can be determined from

$$\begin{aligned} h_l = {} & [0.079393C_l + 156.81]T - 7.452 \times 10^{-5}(100 - C_l)T^2 - 25{,}490C_l T^{-1} \\ & + 228.122C_l + 53{,}769C_l(100 - C_l)/(11{,}869 + 88.51C_l) \\ & - 978.2C_l(100 - C_l)(325.89C_l - 11{,}869)/(11{,}869 + 88.51C_l)^2 - 27{,}747.9 \end{aligned} \tag{21}$$

The local enthalpy relations for the primary α- and γ-phase solids, respectively, are

$$\begin{aligned} h_\alpha = {} & [113.678 + 0.682376C_\alpha]T + [2.3507 \times 10^{-2} + 5.2996 \times 10^{-5}C_\alpha]T^2 \\ & + 214.25C_\alpha + 47{,}590C_\alpha(100 - C_\alpha)/(11{,}869 + 88.51C_\alpha) \\ & - 22{,}930C_\alpha(100 - C_\alpha)(325.89C_\alpha - 11{,}869)/(11{,}869 + 88.51C_\alpha)^2 - 36{,}028 \end{aligned} \tag{22}$$

and

$$\begin{aligned} h_\gamma = {} & [113.678 + 0.682376C_\alpha]T + [2.3507 \times 10^{-2} + 5.2996 \times 10^{-5}C_\alpha]T^2 \\ & - 273.6C_\gamma + 196{,}930C_\gamma(100 - C_\gamma)/(11{,}869 + 88.51C_\gamma) - 33{,}670 \end{aligned} \tag{23}$$

In the above equations the temperature is in kelvins, the concentrations are in wt.% Sn, and the enthalpies are in joules per kilogram. These equations were obtained by weighting the enthalpies of pure lead and pure tin with the atom fraction of each substance and including the heat of mixing. The α-phase solid enthalpy expression, equation (22), was linearized in concentration as mentioned in the section on enthalpy relations. The use of this partially linearized enthalpy function was necessary only for the Scheil model, but

it was also used for the Lever Rule model to allow comparisons between the two models. The error in h_α introduced by the linearization was less than 1% for the range of concentrations considered. No error ranges were provided for equations (21)–(23).[1] Slight inaccuracies in the enthalpy relationships are not expected to have a major impact on the comparisons presented in this paper.

A total of 15 numerical simulations were performed, and the different simplifications made in each of the 15 numerical test cases are summarized in *Table 2*. Cases 2–5 examine the effects of setting the derivatives of the enthalpies with respect to temperature and concentration either to a constant or to zero. Cases 7 and 8 use the same enthalpy relations as cases 1 and 3 but have different thermal initial and boundary conditions. Cases 4 and 5 show the consequences of using the additional simplifications of linearizing the phase diagram or using the same thermophysical properties for the α-phase and eutectic solids. Case 6 investigates the consequences of neglecting microscopic enthalpy variations within the averaging volume.

The constant values for the enthalpy derivatives used in cases 2–5 and case 8 were obtained by averaging the variable properties over the range of temperatures and concentrations through which an averaging volume would pass in completely solidifying, that is, the liquid temperature and concentration ranging from the liquidus to eutectic temperature and the initial to eutectic concentration, respectively. While the choice of these average values for the enthalpy derivatives is somewhat subjective, the method used is reasonable. The only way to choose the "best" average values would be to adjust them until the best agreement between the variable and constant value simulations was achieved; however, this would not be possible in practice. The constant values of the enthalpy derivatives, along with the phase thermal conductivities and densities, are listed in *Table 3*. Case 4 utilized a linear phase diagram in which the liquidus slope and segregation coefficient were constant at -2.284 K/wt.% Sn and 0.3067, respectively. This liquidus slope was obtained by assuming that the liquidus curve is a straight line between the liquidus temperature at a concentration of Pb-20 wt.% Sn and the eutectic temperature and concentration. The segregation coefficient is the value obtained by assuming that both the liquidus and solidus curves are straight lines with the endpoints given by the equilibrium phase diagram. In case 5, all of the solid properties were taken as a weighted average of the α- and γ-phase solid properties. The weighting was based on the volume fractions of the solid phases that were present when the averaging volume was completely solidified.

Results

A comparison of the results for the Lever Rule model cases at two different times is presented in *Table 4*. A similar comparison is made for the Scheil model cases in *Table 5*. Cases 1L and 1S were chosen as reference cases, since no restrictions or changes have been made to the original models. *Table 6* compares the results of the Lever rule and Scheil model cases when the complete enthalpy expressions are used. *Tables 7* and *8* compare the Lever Rule and Scheil model cases with different initial and boundary conditions in a manner similar to that of *Tables 4* and *5*. All of the results are shown at two times to illustrate the fact that the percent differences between the various cases stay approximately the same over time. In all cases the locations of the eutectic and liquidus isotherms are used as the basis of the comparisons.

Table 2. Conditions for each test case

Case	$\left.\frac{\partial\langle h_k\rangle^k}{\partial T}\right\|_{\langle C_k\rangle^k}$	$\left.\frac{\partial\langle h_k\rangle^k}{\partial\langle C_k\rangle^k}\right\|_{\langle T_k\rangle^k}$	Temperature-volume fraction relation	Initial condition, T_0 (K)	Boundary condition, T_{wall} (K)
1L/1S	Variable	Variable	Lever/Scheil	602	356
2L/2S	Constant	Constant	Lever/Scheil	602	356
3L/3S	Constant	0	Lever/Scheil	602	356
4L/4S	Same as 3L/3S but with linearized phase diagram				
5L/5S	Same as 3L/3S but with α- and γ-phase solid properties equal				
6S	Same as 1S but with interfacial solid concentration, rather than average solid concentration, used to calculate α-phase solid enthalpy				
7L/7S	Same as 1L/1S			552	300
8L/8S	Same as 3L/3S			552	300

Table 3. Values of constant or average properties used in various test cases[1,5,7]

Phase	$\left.\frac{\partial\langle h_k\rangle^k}{\partial T}\right\|_{\langle C_k\rangle^k}$ (J/kg/K)	$\left.\frac{\partial\langle h_k\rangle^k}{\partial\langle C_k\rangle^k}\right\|_{\langle T_k\rangle^k}$ (J/kg/wt.% Sn)	Density (kg/m^3)	Thermal conductivity (W/m/K)
Liquid	183.0	210.0	9,400	21.0
α-phase solid	151.0	652.0	10,300	36.0
γ-phase solid	156.5	—	9,750	45.2

Table 4. Comparison of the Lever Rule model cases with case 1L

(a) At t = 65 sec

Case	Location of eutectic isotherm (mm)	Percent change from case 1L	Location of liquidus isotherm (mm)	Percent change from case 1L
1L	22.7	0.0%	49.8	0.0%
2L	21.4	−5.8%	45.8	−8.0%
3L	20.3	−10.8%	44.2	−11.2%
4L	20.6	−9.2%	45.0	−9.6%
5L	20.3	−10.7%	44.3	−11.1%

(b) At t = 110 sec

Case	Location of eutectic isotherm (mm)	Percent change from case 1L	Location of liquidus isotherm (mm)	Percent change from case 1L
1L	29.5	0.0%	65.0	0.0%
2L	27.9	−5.3%	60.2	−7.3%
3L	26.4	−10.5%	57.5	−11.5%
4L	26.6	−10.7%	58.5	−9.9%
5L	20.3	−9.6%	57.6	−11.0%

Table 5. Comparison of the Scheil model cases with case 1S

(a) At t = 65 sec

Case	Location of eutectic isotherm (mm)	Percent change from case 1S	Location of liquidus isotherm (mm)	Percent change from case 1S
1S	22.2	0.0%	49.0	0.0%
2S	21.1	−4.9%	46.3	−5.6%
3S	21.0	−5.4%	45.6	−7.0%
4S	21.4	−3.7%	46.4	−5.3%
5S	21.2	−4.6%	45.7	−6.8%
6S	23.1	+4.2%	49.9	+1.8%

(b) At t = 110 sec

Case	Location of eutectic isotherm (mm)	Percent change from case 1S	Location of liquidus isotherm (mm)	Percent change from case 1S
1S	29.0	0.0%	63.5	0.0%
2S	27.9	−3.8%	60.1	−5.4%
3S	27.6	−4.7%	59.3	−6.6%
4S	28.0	−3.3%	60.4	−5.0%
5S	27.8	−4.1%	59.4	−6.5%
6S	29.8	+2.9%	64.9	+2.1%

Lever Rule model cases

In case 2L the enthalpy derivatives with respect to both temperature and concentration are held constant at the values given in *Table 3*. Therefore the phase enthalpies are linear functions of temperature and concentration. As the results in *Table 4* show, the location of the eutectic and liquidus isotherms is underpredicted by about 5.5% and 7.5%, respectively, in comparison with case 1L.

The assumptions of constant specific heats and no concentration dependence of the enthalpies are often used in modelling heat transfer during solidification,[2,8–10] but the results of case 3L illustrate that these assumptions can significantly alter the resulting heat transfer predictions in the present alloy system. In this case the concentration derivatives of the enthalpies are set to zero, and the temperature derivatives of the enthalpies are held constant. Therefore the phase enthalpies are a linear function of temperature only. The deviations from the predictions of case 1L are about −11% for both the eutectic and liquidus isotherms.

In addition to the simplifications of constant specific heats and no concentration dependence of the phase enthalpies, the assumptions that the equilibrium phase diagram is linear (case 4L) and that the eutectic and α-phase solids have the same thermophysical properties (case 5L) were investigated. Interestingly, the results of case 4L, when compared with the results of case 3L, show that the additional simplification of a linear phase diagram partially offsets the differences introduced by assuming no concentration dependence

of the enthalpies. The deviations from the predictions of case 1L for the movement of the eutectic and liquidus isotherms for case 4L are slightly lower than the deviations of case 3L. In case 5L, in which the phase diagram is nonlinear but the α- and γ-phase properties are assumed to be equal, the differences from case 1L are about -10.1% and -11% for the movement of the eutectic and liquidus isotherms, respectively; this is not significantly different from the results of case 3L. This is expected, since the average solid properties are weighted by the solid volume fractions, and for the Lever Rule model the α-phase volume fraction is 97.4% upon complete solidification.

Scheil model cases

In case 2S the enthalpy derivatives with respect to both temperature and concentration are held constant, and the changes in the prediction of the locations of the eutectic and liquidus isotherms in comparison with case 1S are about -4.3% and -5.5%, respectively. These changes are smaller than the same comparison between cases 2L and 1L. However, this is expected, since

Table 6. Comparison of the Scheil and Lever Rule models

(a) At t = 65 sec

Case	Location of eutectic isotherm (mm)	Percent change from case 1S	Location of liquidus isotherm (mm)	Percent change from case 1S
1S	22.2	0.0%	49.0	0.0%
1L	22.7	2.3%	49.8	1.6%

(b) At t = 110 sec

Case	Location of eutectic isotherm (mm)	Percent change from case 1S	Location of liquidus isotherm (mm)	Percent change from case 1S
1S	29.0	0.0%	63.5	0.0%
1L	29.5	1.6%	65.0	2.2%

Table 7. Comparison of the Lever Rule model cases with different initial and boundary conditions

(a) At t = 65 sec

Case	Location of eutectic isotherm (mm)	Percent change from case 7L	Location of liquidus isotherm (mm)	Percent change from case 7L
7L	33.8	0.00%	119.5	0.0%
8L	30.0	−11.3%	101.1	−15.4%

(b) At t = 110 sec

Case	Location of eutectic isotherm (m)	Percent change from case 7L	Location of liquidus isotherm (mm)	Percent change from case 7L
7L	44.0	0.0%	154.1	0.0%
8L	39.0	−11.3%	129.9	−15.7%

Table 8. Comparison of the Scheil model cases with different initial and boundary conditions

(a) At t = 65 sec

Case	Location of eutectic isotherm (mm)	Percent change from case 7S	Location of liquidus isotherm (mm)	Percent change from case 7S
7S	32.8	0.0%	114.9	0.0%
8S	30.8	−5.9%	99.1	−13.7%

(b) At t = 110 sec

Case	Location of eutectic isotherm (mm)	Percent change from case 7S	Location of liquidus isotherm (mm)	Percent change from case 7S
7S	42.5	0.0%	148.2	0.0%
8S	40.1	−5.7%	127.1	−14.2%

accounting for the microscopic concentration gradients in the solid for the Scheil model causes the average solid concentration to take a smaller range of values than for the Lever Rule model. Therefore the concentration effects on the solid enthalpy and its derivatives is smaller for the Scheil model. In addition, the Scheil model predicts a much larger volume fraction of α-phase solid, at 85.6%, than does the Lever Rule model. Since there is much more eutectic solid and the eutectic enthalpy is a function of temperature only, the concentration dependence of the predictions is further reduced.

Case 3S shows the consequences of ignoring the dependence of the enthalpies on concentration by making them linear functions of temperature only. The differences in the movement of the eutectic and liquidus isotherms between cases 1S and 3S are smaller than the differences between cases 1L and 3L. This can also be attributed to the effects of accounting for the microscopic concentration profile in the solid and the larger eutectic solid fraction when using the Scheil model.

As was mentioned in the discussion of cases 4L and 5L, the additional assumptions of a linear phase diagram or equal properties for the α- and γ-phase solids are often used to simplify the solution of alloy phase change problems. *Table 5* shows that for case 4S, in which the linearized phase diagram is used, the deviations from case 1S are around -4%, indicating, as did case 4L, a slight improvement. Case 5S shows the effects of using equal α- and γ-phase properties. Again, one can observe a slight improvement in the prediction of the movement of the eutectic and liquidus isotherms over those of case 3S. This is different from the results of case 5L but is expected, since the eutectic solid fraction, which is used to weigh the solid properties, is much larger for the Scheil model.

Case 6S illustrates the consequences of neglecting the effects of the microscopic concentration profile in the solid on the enthalpy. Here, the *interfacial* solid concentration rather than the *average* solid concentration was used in calculating the α-phase solid enthalpy and its derivatives. Note that this will produce differences only for the Scheil model, since the Lever Rule model assumes that the average and interfacial solid concentrations are equal. *Table 5* shows that case 6S is the only case that overpredicts the penetration of the eutectic and liquidus isotherms, the differences from case 1S being about 2%.

Lever Rule-Scheil model comparison

Table 6 shows that, in comparison with the Scheil model, the penetration of the eutectic and liquidus isotherms is about 2% faster for the Lever Rule model. One reason for this difference is the fact that the Scheil model gives a much lower solid volume fraction when the eutectic temperature is reached. On the average, the eutectic solid has a larger average liquid-solid enthalpy difference than does the α-phase solid, so more heat needs to be removed to form the eutectic solid than the α-phase solid.

Different initial/boundary conditions

Cases 7 and 8 used the same enthalpy relations as cases 1 and 3, but the initial temperature was reduced by 56 K, and the boundary temperature was reduced by 50 K. This made the initial temperature only a fraction of a degree higher than the liquidus temperature. A comparison of cases 7L and 8L in *Table 7* shows that the locations of the eutectic and liquidus isotherms in case 8L were underpredicted by about 11.3% and 15.5%, respectively. The same comparison between cases 1L and 3L in *Table 4* shows that the change in the locations of the eutectic isotherm is nearly the same, while the change in the movement of the liquidus isotherm is somewhat larger with the different initial and boundary conditions. A similar comparison between cases 7S/8S and cases 1S/3S, in *Tables 8* and *5*, shows similar results for the Scheil model cases. This indicates that the results shown in *Tables 4–6* are relatively independent of the thermal initial and boundary conditions. This can be expected because the solidification temperature range is fixed for an alloy of a given composition.

Conclusions

The effects of using enthalpy relations that are functions of both temperature and concentration on the heat transfer during the solidification of a Pb-20 wt.% Sn alloy were observed by performing several numerical test cases using a volume-averaged mixture model. The relationship between the solid fraction and temperature was defined by two limiting cases: the Lever Rule model and the Scheil model. When the derivatives of the enthalpy with respect to concentration and temperature were assumed to be constant, the movement of the eutectic and liquidus isotherms was significantly underpredicted in comparison to a case in which the enthalpy derivatives were allowed to vary with both concentration and temperature. Ignoring the concentration dependence of the enthalpy completely caused an even larger error. When the phase diagram was assumed to be linear or the α- and γ-phase solids were assumed to have the same properties while the enthalpies were assumed to be linear functions of the temperature only, the predictions were slightly improved. When the microscopic concentration variations in the solid due to the Scheil model were ignored in calculating the average solid enthalpy, the isotherm movement was overpredicted by about 2%. This study considered a relatively large concentration of 20 wt.% Sn only, to emphasize the errors introduced by the various simplifications and because the Pb-20 wt.% Sn alloy has been a popular choice in low-temperature solidification experiments.[1,5,6] The errors in the heat transfer predictions due to the neglect of the concentration dependence of the enthalpies can be expected to decrease with lower initial concentrations. Finally, the results were shown to be relatively independent of the thermal initial and boundary conditions.

Although fluid flow was not accounted for and the relatively simple case of solidification in a semi-infinite domain was considered, the present results should serve

as an estimation of the magnitude of the changes in the heat flow introduced by simplifying enthalpy relations and neglecting the microscopic concentration profile in the solid. These differences may be considerably magnified when fluid flow is included because they will affect the thermal and solutal buoyancy forces within the mushy zone.

The present paper also indicates a need to develop and utilize complete enthalpy relationships of the form of equations (21)–(23) for other alloys. As was mentioned by Poirier and Nandapurkar,[1] considerable progress has been made during the recent decade to summarize thermodynamic state functions of numerous alloys. Although not investigated within the context of this study, it appears that the use of a proper energy equation and accurate state functions is necessary to obtain good agreement between predictions and measurements in alloy solidification.

Acknowledgments

The authors gratefully acknowledge support for this work by the National Science Foundation under grant CBT-8808888.

Nomenclature

C concentration (wt.% Sn)
f segregation coefficient equation
g liquidus curve equation
h enthalpy (J/kg)
k thermal conductivity (W/m/K)
t time (s)
T temperature (K)
V volume (m^3)
X atom fraction

Greek symbols
ϵ volume fraction
κ segregation coefficient
ρ density (kg/m^3)
X_k phase function
Ψ_k a quantity of a phase

Subscripts
α alpha phase
γ gamma phase
i interfacial
k phase k
l liquid
0 averaging, initial
Pb lead
s solid
Sn tin

Superscript
lin partially linearized

References

1 Poirier, D. R. and Nandapurkar, P. Enthalpies of a binary alloy during solidification. *Metall. Trans. A* 1988, **19A**, 3057–3061
2 Beckermann, C. and Viskanta, R. Double-diffusive convection during dendritic solidification of a binary mixture. *Physico-Chem. Hydrodynamics* 1988, **10**, 195–213
3 Ni, J. and Beckermann, C. A two-phase model for mass, momentum, heat, and species transport during solidification. *Transport Phenomena in Materials Processing*, HTD-VOL. 132, ed. M. Charmichi, M. K. Chyu, Y. Joshi and S. M. Walsh. ASME, New York, 1990, pp. 45–56
4 Kurz, W. and Fisher, D. J. *Fundamentals of Solidification*. Trans Tech, Aedermannsdorf, Switzerland, 1986, pp. 129–130
5 Poirier, D. R. Densities of Pb-Sn alloys during solidification. *Metall. Trans. A* 1988, **19A**, 2349–2354
6 Chisea, F. M. and Guthrie, R. I. L. Natural convection heat transfer during the solidification and melting of metals and alloy systems. *ASME J. Heat Transfer* 1974, **96**, 377–384
7 Touloukain, Y. S., Powell, R. W., Ho, C. Y. and Klemens, P. G. *Thermophysical Properties of Matter*, Vol. 1. IFI/Plenum, New York, 1970, pp. 652–654
8 Prakash, C. Two-phase model for binary solid-liquid phase change. Part 1: Governing equations. *Numer. Heat Transfer B* 1990, **18B**, 131–145
9 Bennon, W. D. and Incropera, F. P. A continuum model for momentum, heat and species transport in binary solid-liquid phase change systems. I: Model formulation. *Internat. J. Heat Mass Transfer* 1987, **30**, 2161–2170
10 Voller, V. and Prakash, C. On the numerical solution of continuum mixture model equations describing binary solid-liquid phase change. *Numer. Heat Transfer B* 1989, **15**, 171–189